A miniature 7g jumping robot

Mirko Kovač, Martin Fuchs, André Guignard, Jean-Christophe Zufferey, Dario Floreano
Ecole Polytechnique Fédérale de Lausanne (EPFL)
Laboratory of Intelligent Systems (LIS, http://lis.epfl.ch)
CH-1015 Lausanne, Switzerland
{mirko.kovac, m.fuchs, andre.guignard, jean-christophe.zufferey, dario.floreano}@epfl.ch

***Abstract*— Jumping can be a very efficient mode of locomotion for small robots to overcome large obstacles and travel in natural, rough terrain. In this paper we present the development and characterization of a novel 5cm, 7g jumping robot. It can jump obstacles more than 27 times its own size and outperforms existing jumping robots by one order of magnitude with respect to jump height per weight and jump height per size. It employs elastic elements in a four bar linkage leg system to allow for very powerful jumps and adjustment of the jumping force, take-off angle and force profile during the acceleration phase.**

I. INTRODUCTION

Small robots have big problems when it comes to efficient locomotion in natural and rough terrains. This effect is usually referred to as the "Size Grain Hypothesis" [1], which is described as an "increase in environmental rugosity with decreasing body size". One possibility to tackle this problem is to adopt a jumping mechanism.

The main advantages of using jumping as a principle mode of locomotion for small scale systems are (i) the ability to overcome large obstacles [2][3], (ii) its energetic efficiency compared to other locomotion methods such as crawling, walking or running [4][5] and (iii) the possibility to use a light weight low force actuator to slowly charge an elastic element and obtain very powerful jumps after release [6][7][8].

This paper presents the development and characterization of a versatile 7g jumping mechanism (figure 1) that can overcome obstacles of around 1.4m height. It is adjustable in take-off angle, jumping height and force profile during the jump and is designed to accommodate different types of bodies and payloads (see a movie of the prototype in the accompanying video material).

To date, there have been several projects on jumping robots (see table I for an overview of jumping robots with on-board energy and control) for different applications and weights. The most closely related jumping device to the mechanism presented here in terms of weight and size is the Grillo project [9]. However, the prototypes presented so far jump distances of only a few centimeters.

In the following sections, we first introduce the underlying calculations of jumping force and energy, outline our design methodology, present its implementation in Computer Aided Design (CAD) and optimization using Finite Element Analysis (FEA). Finally we describe the working prototype and characterize its jumping performance.

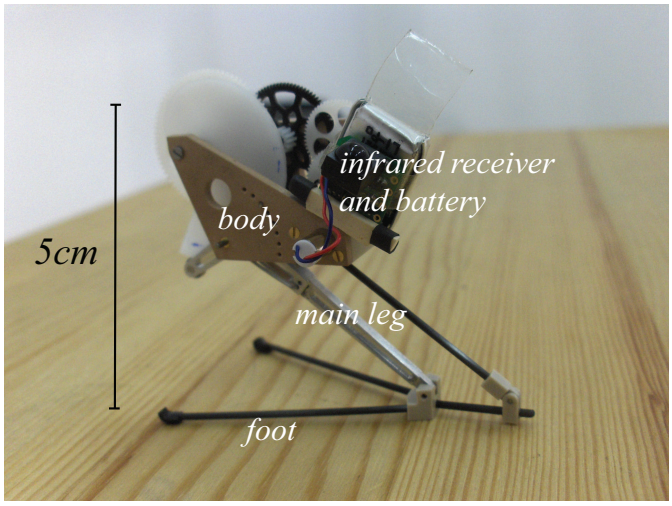

Fig. 1. 7g jumping mechanism prototype capable of overcoming obstacle of up to 1.4m height.

II. DESIGN

In order to design and adequately dimension the structural parts of our jumping robot, we estimated the required energy for jumping and the forces acting on the system. As a performance benchmark, we decided to design the system to be capable of overcoming an obstacle of 1m height h at a takeoff angle α_0 of 75°with a total system mass m of 10g (figure 2).

Moreover, to be able to optimize the efficiency of the transmission of energy from the legs to jumping height, we have to design the mechanism that can translate the input torque into a designable vertical and horizontal force profile on the ground. This is very important for light weight robots to prevent forces from being too high at the beginning of the acceleration phase which can cause the system to take-off before all the energy has been released [5]. It also can facilitate jumps on slippery surfaces where too much horizontal force at the beginning of the jump may lead to friction problems [13]. Therefore, we choose to implement a four bar linkage design for the legs (figure 3). Using this design offers the possibility to modify the take-off angle by adjustment of distance *(e)*, the acceleration time by adjustment of distances *(a)* and *(c)* and the trajectory of the foot tip P by adjustment of the ratio *(b)/(d)* (figure 4).

Based on the calculations of the forces acting on the

TABLE I

STATE OF THE ART ON JUMPING ROBOTS WITH ON BOARD ENERGY AND CONTROL

Name	mass [g]	approx. jump height [cm]	jump height per mass [cm/g]	approx. jump height per size [-]
Rescue robot [10]	2000	80	0.04	3.5
Minimalist jumping robot [11]	1300	90	0.07	6
Jollbot [5]	465	21.8	0.05	1.4
Scout [12]	200	35	0.18	3.5
Mini-Whegs [3]	190	22	0.12	2.2
Grillo [9]	8-80	5	0.63-0.06	1
Jumping robot presented here	**7**	**138**	**19.77**	**27.6**

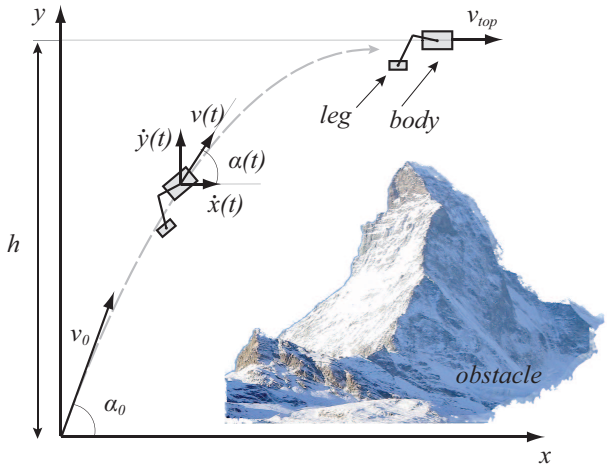

Fig. 2. Sketch of the jump. Jumping height h, take-off angle α_0, take-off velocity v_0 horizontal $\dot{x}(t)$ and vertical $\dot{y}(t)$ velocity during flight and horizontal velocity on the top of the jumping trajectory v_{top}.

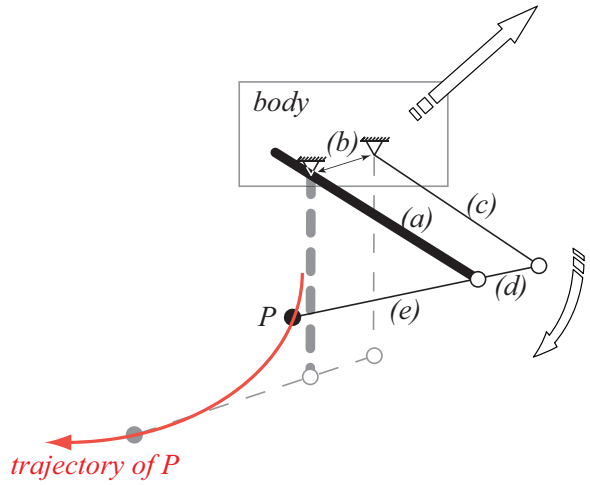

Fig. 3. Sketch of the four bar linkage jumping design and the foot tip P trajectory during take-off. *(a)* is the input link and *(b)* the ground link. Changing the lengths (a)-(d) allows to adjust the take-off angle (change distance (e)), acceleration time (change distance (a) and (c)) and trajectory of the foot tip P (change ratio (b)/(d).

system we designed the components of the four bar linkage and the body in CAD (figure 5 and 6) and optimized the critical part (main leg, figure 1) using FEA (figure 7).

A. Jump energy

Based on ballistic jump kinematics, the force balance on the system during jump (figure 2) can be expressed as:

$$F_x(t) = -F_{air}(t) \cdot cos(\alpha(t)) \tag{1}$$

$$F_y(t) = -F_{air}(t) \cdot sin(\alpha(t)) - F_g \tag{2}$$

with $F_x(t)$ being the horizontal and $F_y(t)$ the vertical force component, F_g the weight, $F_{air}(t)$ the air friction and $\alpha(t)$ the angle of the flight direction.

As a first model of the air friction force $F_{air}(t)$ we assume [14]:

$$F_{air}(t) = \frac{1}{2}\rho v^2(t) A c_d \tag{3}$$

with ρ as the air density, $v(t)$ the velocity of the system, A the frontal area and c_d the drag coefficient.

Using these equations and the trigonometric relationship

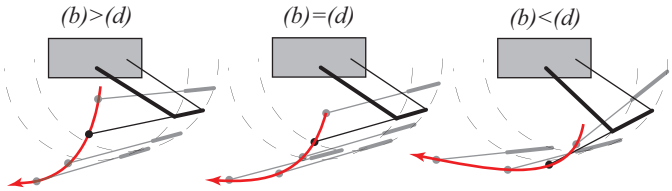

Fig. 4. Trajectory of foot tip P for three different ratios (b)/(d) (figure 3).

$$\alpha(t) = \arctan(\frac{\dot{y}(t)}{\dot{x}(t)}) \tag{4}$$

we obtain a system of two nonlinear second order differential equations with $\dot{x}(t)$ being the horizontal and $\dot{y}(t)$ the vertical velocity. Accordingly, $\ddot{x}(t)$ is the horizontal and $\ddot{y}(t)$ the vertical acceleration:

$$\ddot{x}(t) = -\frac{1}{2m}\rho A c_d \cos(\arctan(\frac{\dot{y}(t)}{\dot{x}(t)})) \cdot (\dot{x}(t)^2 + \dot{y}(t)^2) \tag{5}$$

$$\ddot{y}(t) = -\frac{1}{2m}[2mg + \rho A c_d \sin(\arctan(\frac{\dot{y}(t)}{\dot{x}(t)})) \cdot (\dot{x}(t)^2 + \dot{y}(t)^2)] \tag{6}$$

The initial conditions can be expressed as:

$$\dot{x}(0) = cos(\alpha_0) \cdot v_0 \tag{7}$$

$$\dot{y}(0) = sin(\alpha_0) \cdot v_0 \tag{8}$$

$$x(0) = 0 \tag{9}$$

$$y(0) = 0 \tag{10}$$

However, the frontal area A and the drag coefficient c_d are not known exactly, a priori, and have to be estimated. The fact that our robot is very similar to jumping animals such as desert locusts, allows us to adopt data from animal studies to provide a first approximation. We model the robot as a cylindrical body (length l of 100mm and radius r of 40mm), as suggested by Bennet-Clark [7] and used for locusts. Assuming the flight direction in line with the body axis, a take-off angle α of 75°, a friction coefficient c_d of 1.3 [7] and an air density ρ of 1.2kg/m^3 we solved this system of differential equations numerically using a Runge-Kutta (4,5) solver [15] and obtained a required take-off velocity v_0 of 4.05m/s.

This corresponds to an initial kinetic energy E_{kin0} of

$$E_{kin0} = \frac{1}{2}mv^2 = 82mJ \tag{11}$$

Introducing a security factor that accounts for eventual additional losses in the leg structure and consulting available off the shelf components, we decided to design the system for an energy of up to 154mJ.

Based on this energy, the acceleration phase and forces acting on the system can be estimated. If we assume constant acceleration and an approximate acceleration distance of 3cm to discharge 154mJ, we obtain a force of 5.1N acting on the system for a duration of 10.8ms. This approximation of force and energy was used for the dimensioning phase that follows.

The total system mass of 10g as assumed in the beginning consists of the jumping mechanism including battery, electronics and as much payload as possible. It is thus of interest to decrease the weight of the actual jumping mechanism in order to either allow for more payload or jump higher with the same payload (equation 11). Another important issue is the distribution of mass between the leg and the main body. This influence can be described with the help of the so called 'cost of transport' T [4] which is defined as the kinetic energy of a jumping system divided by the mass and distance of a jump. It can therefore be used as an indicator for the jumping efficiency. With m as the mass of the entire system, $a \cdot m$ as the leg mass and $(1-a) \cdot m$ as the body mass we can express the cost of transport as (figure 8):

$$T = \frac{g}{2(1-a)\sin(2\alpha)} \tag{12}$$

Reducing the fraction a, even slightly, allows us to decrease the cost function T and obtain an efficient jumping mechanism. Hence, we optimized the leg structure using FEA on the main leg (figure 1).

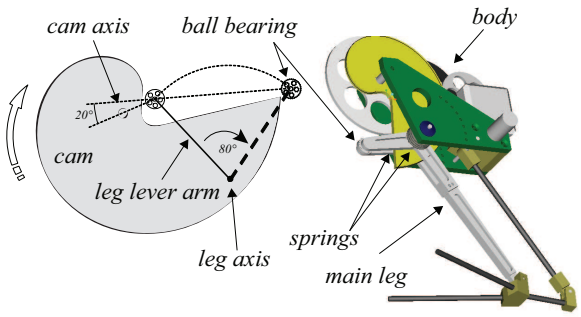

Fig. 5. Cam that charges the two torsion spring and CAD model of the jumping mechanism.

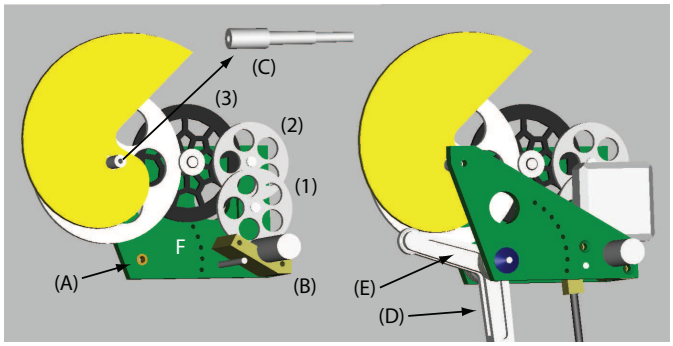

Fig. 6. CAD model of the gearbox. (A) brass bearing to reduce friction, (B) distance piece to align the two body plates, (C) cam axis, (D) slot in main leg for the cam, (E) main leg and, (F) series of holes for spring setting. (1),(2) 0.2mm POM gears and (3) 0.3mm POM gear

B. Mechanical design

As calculated, during the acceleration phase, an energy of 154mJ has to be released in only 10.8ms, which corresponds to 14.2W. Since there is no actuator capable of producing that much power at a weight of only a few grams, we decided to design a mechanisms which can be charged slowly, store the energy in a spring and release it on demand using a click mechanism. This mechanical principle is used by several small jumping animals, such as frogs [6], locusts [7], springtails [16], click beatles [4] and fleas [8].

Two torsion springs, used as elastic elements, are located on the leg axis which are connected to the main leg and the body (figure 5). To charge these two springs, a small (0.66g 4mm DC) pager motor actuates a cam and rotates the leg lever arm by 80°for one charge cycle. The shape of the cam has been specifically designed to yield a constant torque on the motor through a four stage gearbox system. In order to keep the weight as low as possible, we choose two 0.2mm gears with 60 teeth (figure 6 (1) and (2)) and a third stage 0.3mm gearwheel (3) with 81 teeth. This resulted in a total gear weight of 0.63g with an overall efficiency of 61% (assuming an efficiency of 85% for each stage). The total transmission ratio is 1266 and allows for motor speeds of around 8000t/min with a constant motor torque of only 0.038mNm.

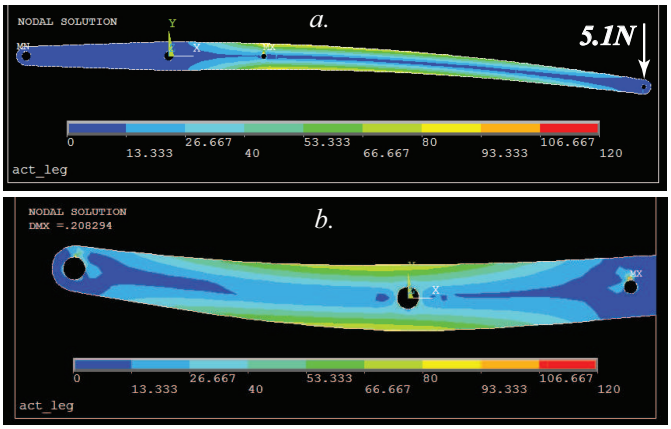

Fig. 7. Results of the FEA on a simplified 2D model of the main leg. a. Stress at take-off, max. von Mises stress $\sigma_m \approx 90MPa$, max. deflection $d = 0.9mm$, b. Stress in charged position, max. von Mises stress $\sigma_m \approx 85MPa$, max. deflection $d = 0.21mm$.

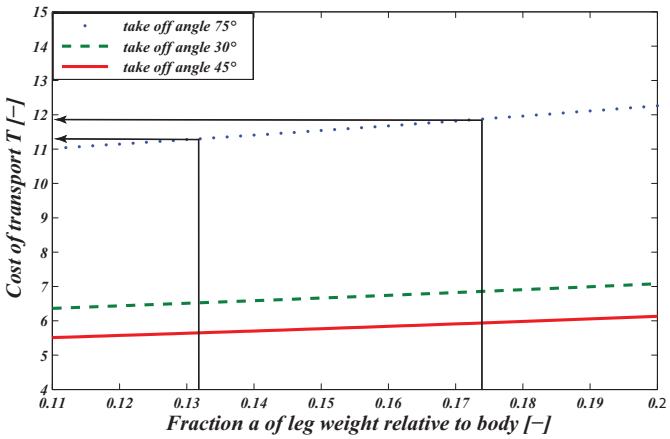

Fig. 8. Cost function for different relative masses of the leg $a \cdot m$ in regard to the body mass $(1-a) \cdot m$ at different take-off angles.

C. Structure optimization using FEA

According to structural mechanics [17], when using aluminium for the main leg material, we determined that a diameter of 2.2mm is needed to support the force of 5.1N where we assume a uni-axial stress condition, a leg length of 4cm and a security factor of 1.2. In order to minimize the leg weight while keeping its required strength, we performed a 2D FEA on a simplified model of the main leg using commercial FEA software (ANSYS). The analysis indicates that the main stress lies close to the axis and on the surface perpendicular to the force vector (figure 7). Therefore, we removed the unnecessary material in the middle section of the leg to obtain a structurally beneficial H-shape which lead to a mass reduction of the main leg from 0.99g to 0.76g (23.2%). This also reduced the fraction a (equation 12) by 23.4% from 0.174 to 0.132. Thus, an improvement of the cost function of 4.7% (figure 8) has been obtained for the jumping mechanism by optimizing the shape and weight of the main leg.

TABLE II
PROPERTIES OF THE MATERIALS USED

	Alu	PEEK	POM	Carbon	Cibatool
Density [g/cm^3]	2.7	1.3	1.56	1.55	0.7
E-Module [GPa]	69	3.5	5.2	130	N/A
Yield strength [MPa]	320	97	62	1400	25-30

TABLE III
WEIGHT BUDGET

Part	material	weight [g]
Body frame	Cibatool/PEEK	1.4
Cam	POM	0.78
Gears	POM	0.63
Main leg	Aluminium	0.76
Plastic parts on leg	PEEK/Carbon	0.32
Screws and axis	Steel/brass	0.79
2 springs	Spring steel	0.41
Motor		0.65
Total mass mechanism		**5.74**
LiPo Battery		0.48
IR receiver		0.76
Total mass prototype		**6.98**

III. RESULTS

A. Prototype

The prototype (figure 1) consists of the gearbox including motor, gearwheels and cam, the main leg, 1.3mm carbon rods as feet, the infrared receiver and a 10mAh Lithium Polymer battery. As described earlier, changing the proportions of the feet leads to a change in take-off angle, acceleration time and foot trajectory. The amount of energy that will be stored in the springs can be adjusted by changing the spring setting (figure 6 (F)) between 106mJ and 154mJ in steps of 6mJ. The two body plates consist of a material called Cibatool. It is commonly used for rapid prototyping, possesses an excellent machinability and low weight. The cam and gears are manufactured from Polyoxymethylene (POM) due to its low weight and low surface friction coefficient. For critical structural parts in the body and legs we used Polyetheretherketone (PEEK) due to its very high strength-to-weight ratio (see table II for a selection of properties of the materials that have been used). Table III presents the weight budget of the robot. The entire and fully functional remote controlled prototype weights 6.98g in its current form. Further weight reduction could be achieved by optimizing the body frame and by using a smaller infrared receiver and battery.

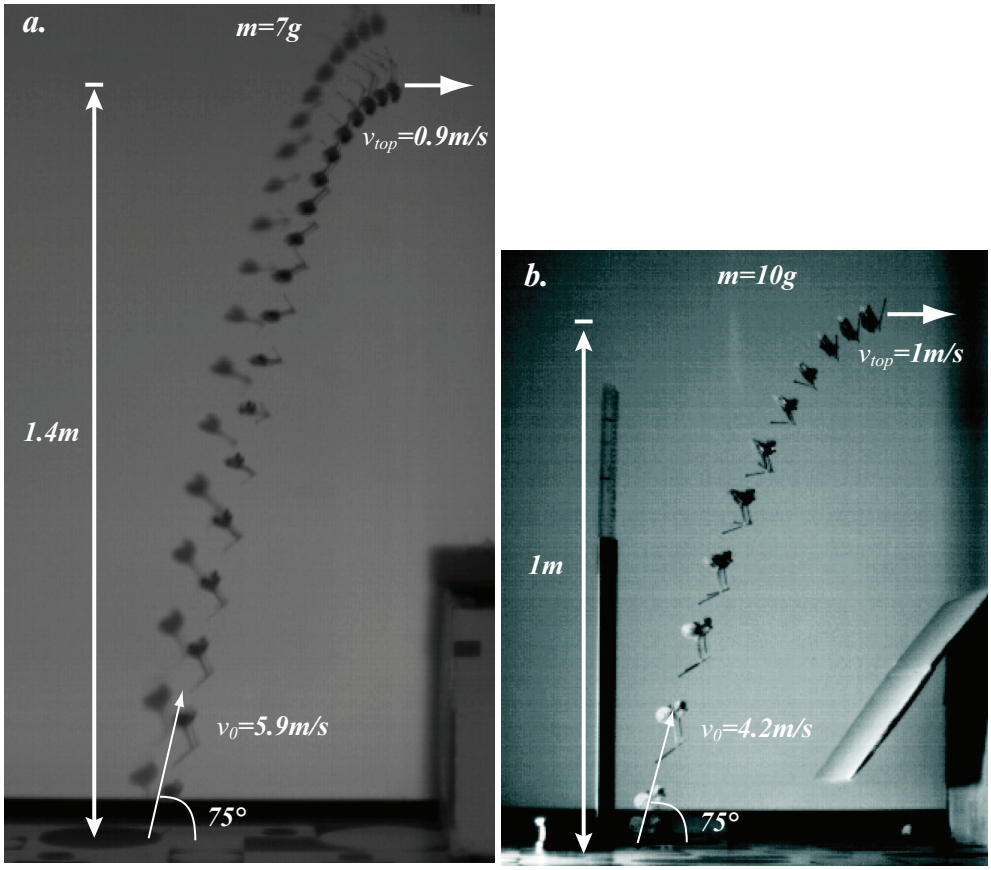

Fig. 9. a. Jumping trajectory of the prototype without and b. with an additional payload of 3g.

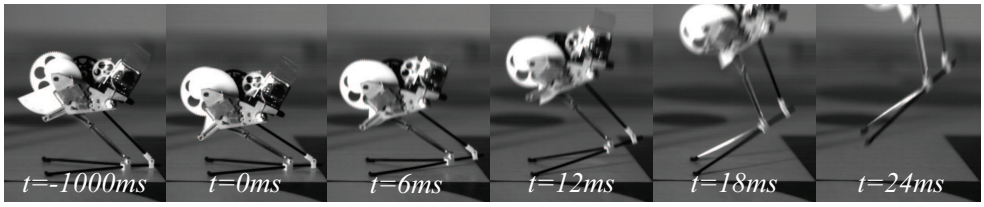

Fig. 10. Takeoff sequence of the jumping mechanism including a payload of 3g.

B. Jumping performance

For the characterization of the jumping performance, we set the leg segment *(a)* and *(c)* to 40mm, *(b)* and *(d)* to 12.5mm and *(e)* to 44mm (figure 3) in order to obtain a take-off angle of 75°and we observed the jumps using a high speed camera running at 1000 frames per second. We recorded the jump of the 7g jumping prototype without additional mass (figure 9 a.) and with additional 3g of lead in order to simulate a payload (figure 9 b.).

The maximal height obtained without additional payload was 138cm. The acceleration time is 15ms, the initial take-off velocity 5.96m/s and the velocity at the top 0.9m/s. The complete jump duration is 1.02s and the traveled distance 79cm. This means that the prototype presented here is capable of overcoming obstacles of more than 27 times its own body size.

The prototype with an additional weight of 3g reached a height of 1.05m with a velocity of 1m/s at the top and an initial take-off velocity of 4.2m/s. This take-off velocity compares very well to the predicted 4.05m/s take-off velocity as modeled in the design phase. However, the acceleration time of 19ms is much longer than the 10.8ms from the prediction. We argue that this is due to a slightly longer acceleration distance of 3.2cm instead of 3cm from the model, inertia effects and friction in the leg axis.

Figure 10 depicts a complete take-off sequence of the

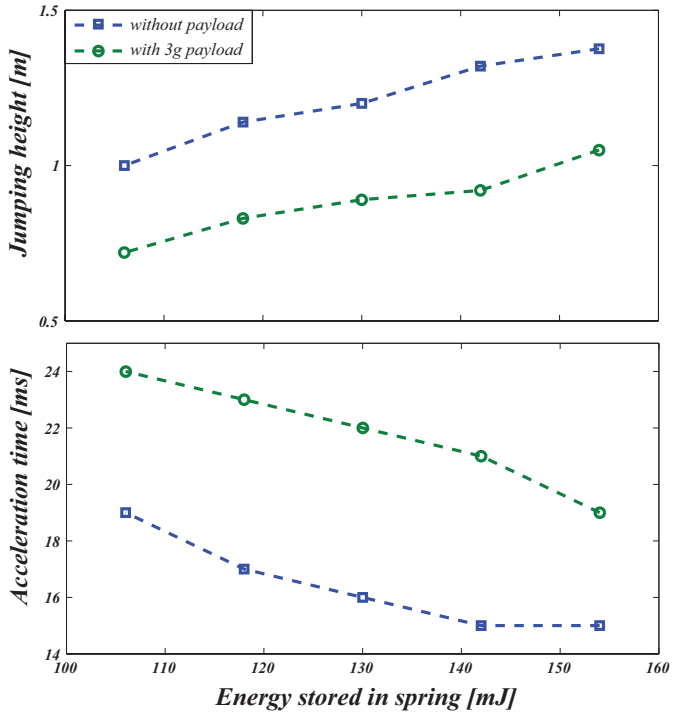

Fig. 11. Jump height and acceleration time at different spring settings for the prototype with and without an additional payload of 3g.

jumping prototype including the 3g payload. In order to illustrate the adaptability of the jumping force, we also characterized the jump height and acceleration time for the two weight setups at different spring settings (figure 11).

The motor recharges the mechanism for one jump cycle in 3.5s while sinking 95mA. This results in a power consumption of 352mW at 3.7V. The 10mAh provided by the LiPo battery would thus theoretically allow for 6.3min of continuous recharging or approximately 108 jumps.

IV. Conclusion

In this paper, we presented a versatile 7g remote controlled jumping robot prototype that has an adjustable take-off angle, jumping force and force profile during take-off. As with many small jumping animals such as frogs, locusts, click beatles and fleas, it charges an elastic element and releases it quickly using a click mechanism so to obtain very powerful jumps. It can jump obstacles more than 27 times its own size and clearly outperforms existing jumping robots with respect to jump height per weight and jump height per size. Using a 10mAh LiPo battery, it can theoretically perform up to 108 jumps which corresponds to a height difference of 148m.

This jumping mechanism could form the propulsion system of a miniature mobile robot or be used for self-deployment of sensors. Our current research efforts aim at combining it with a foldable wing mechanism based on our previously presented 1.5g microglider [18] that would allow the robot to jump and glide towards a desired location.

V. Acknowledgement

The authors would like to thank the Atelier de l'Institut de production et robotique (ATPR), especially Jean-Jacques Crausaz and Pascal Zbinden for their competent advice and endurance in the iterative fabrication process. Also, many thanks to Peter Dürr for the help with the mathematical modeling, Jean-Daniel Nicoud from www.didel.ch and James Roberts for the fruitful discussions and help with mechanical challenges. This project is funded by EPFL.

References

[1] M. Kaspari and M. D. Weiser, "The size-grain hypothesis and interspecific scaling in ants," *Functional Ecology*, vol. 13, no. 4, pp. 530–538, 1999.

[2] U. Scarfogliero, C. Stefanini, and P. Dario, "A bioinspired concept for high efficiency locomotion in micro robots: The jumping robot grillo," in *IEEE International Conference on Robotics and Automation*, 2006, pp. 4037–4042.

[3] B. G. A. Lambrecht, A. D. Horchler, and R. D. Quinn, "A small, insect-inspired robot that runs and jumps," in *International Conference on Robotics and Automation*, 2005, pp. 1240– 1245.

[4] R. M. Alexander, *Principles of Animal Locomotion*. Princeton University Press, 2003.

[5] R. Armour, K. Paskins, A. Bowyer, J. F. V. Vincent, and W. Megill, "Jumping robots: a biomimetic solution to locomotion across rough terrain," *Bioinspiratoin and Biomimetics Journal*, vol. 2, pp. 65–82, 2007.

[6] T. J. Roberts and R. L. Marsh, "Probing the limits to muscle-powered accelerations: lessons from jumping," *Journal of Experimental Biology*, vol. 206, no. 15, pp. 2567–2580, 2003.

[7] H. C. Bennet-Clark, "The energetics of the jump of the locust schistocerca gregaria," *Journal of Experimental Biology*, vol. 63, no. 1, pp. 53–83, 1975.

[8] W. Gronenberg, "Fast actions in small animals: springs and click mechanisms," *Journal of Comparative Physiology A: Sensory, Neural, and Behavioral Physiology*, vol. 178, no. 6, pp. 727–734, 1996.

[9] U. Scarfogliero, C. Stefanini, and P. Dario, "Design and development of the long-jumping "grillo" mini robot," in *IEEE International Conference on Robotics and Automation*, 2007, pp. 467–472.

[10] H. Tsukagoshi, M. Sasaki, A. Kitagawa, and T. Tanaka, "Design of a higher jumping rescue robot with the optimized pneumatic drive," in *IEEE International Conference on Robotics and Automation*, 2005, pp. 1276–1283.

[11] J. Burdick and P. Fiorini, "Minimalist jumping robot for celestial exploration," *The Internation Journal of Robotics Research*, vol. 22, no. 7, pp. 653–674, 2003.

[12] S. A. Stoeter, P. E. Rybski, and N. Papanikolopoulos, "Autonomous stair-hopping with scout robots," in *IEEE/RSJ International Conference on Intelligent Robots and Systems*, vol. 1, 2002, pp. 721–726.

[13] J. Scott, "The locust jump: an integrated laboratory investigation," *Advances in Physiology Education*, vol. 29, no. 1, pp. 21–26, 2004.

[14] P. K. Kundu and I. M. Cohen, *Fluid Mechanics*. Academic Press, 2004.

[15] J. C. Butcher, *The numerical analysis of ordinary differential equations: Runge-Kutta and general linear methods*. Wiley-Interscience New York, 1987.

[16] J. Brackenbury and H. Hunt, "Jumping in springtails: mechanism and dynamics," *Journal of Zoology*, vol. 229, pp. 217–236, 1993.

[17] R. T. Kaftka and Z. Gürdal, *Elements of Structural Optimization*. Kluwer Academic Publishers, 1992.

[18] M. Kovac, A. Guignard, J.-D. Nicoud, J.-C. Zufferey, and D. Floreano, "A 1.5g SMA-actuated microglider looking for the light," in *IEEE International Conference on Robotics and Automation*, 2007, pp. 367–372.